Ballistic Phonon Transport in Holey Silicon

Jaeho Lee,[†,§,⊥,#] Jongwoo Lim,[†,§,#] and Peidong Yang*[,†,‡,§,‖]

[†]Department of Chemistry, [‡]Department of Materials Science and Engineering, University of California, Berkeley, California 94720, United States,

[§]Materials Sciences Division, Lawrence Berkeley National Laboratory, Berkeley, California 94720, United States,

[‖]Kavli Energy Nanosciences Institute, Berkeley, California 94720, United States,

[⊥]Department of Mechanical and Aerospace Engineering, University of California, Irvine, California 92697, United States

Ⓢ Supporting Information

ABSTRACT: When the size of semiconductors is smaller than the phonon mean free path, phonons can carry heat with no internal scattering. Ballistic phonon transport has received attention for both theoretical and practical aspects because Fourier's law of heat conduction breaks down and the heat dissipation in nanoscale transistors becomes unpredictable in the ballistic regime. While recent experiments demonstrate room-temperature evidence of ballistic phonon transport in various nanomaterials, the thermal conductivity data for silicon in the length scale of 10−100 nm is still not available due to experimental challenges. Here we show ballistic phonon transport prevails in the cross-plane direction of holey silicon from 35 to 200 nm. The thermal conductivity scales linearly with the length (thickness) even though the lateral dimension (neck) is as narrow as 20 nm. We assess the impact of long-wavelength phonons and predict a transition from ballistic to diffusive regime using scaling models. Our results support strong persistence of long-wavelength phonons in nanostructures and are useful for controlling phonon transport for thermoelectrics and potential phononic applications.

KEYWORDS: Thermal conductivity, cross-plane, heat transfer, thermoelectric, nanoporous, phononic crystals
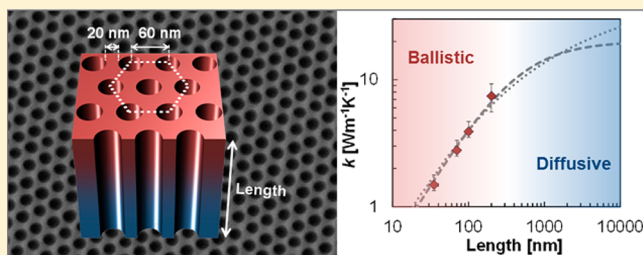
Ballistic phonon transport received large attention for fundamental interests in heat conduction across super-lattices and nanoscale materials.[1,2] When the length scale in the direction of temperature gradient is shorter than the phonon mean free path, phonons can travel through the medium with no internal scattering, which leads to absence of local temperature or thermodynamic equilibrium. The thermal conductivity becomes a property that depends on the system size. The ballistic phonon transport in silicon has great relevance to practical applications[3−7] due to the change in thermal conductivity. Thermal conductivity reduction in silicon nanostructures has been one of the major themes of thermoelectrics in the past decade.[8−15] The vapor−liquid−solid grown nanowires[8−10] provided lateral spatial confinement below the phonon mean free path and reduced the thermal conductivity by an order of magnitude compared to bulk silicon. The crystalline nanowires with induced surface roughness[9−13] demonstrated thermal conductivity approaching the amorphous limit. While many versions of silicon nanowire thermal conductivity data exist, experimental reports showing the length dependence below the phonon mean free path are not available. The average phonon mean free path of silicon at room temperature is known to be around 200−300 nm based on theoretical predictions[1] and thin film experiments.[18] The past thermal conductivity measurement[12] for silicon nanowires of varying length from 3 to 50 μm did not show any appreciable

dependence because of the relatively large length scale. Thermal conductivity of silicon nanowires in submicrometer length scales may show further reduction, which is desirable for thermoelectric applications.

Ballistic phonon transport in silicon is important in nanoelectronics because transistor length scales are actively scaling below the phonon mean free path and the resultant thermal conductivity reduction leads to excessive heat generation.[3,4] The ballistic phonon transport in silicon is also important for potential phononic applications, which are aiming to process information by controlling heat flow.[6,7] The phononic applications have not been explored much because inelastic phonon scattering is considered dominant at room temperature and destroys wave characteristics or information processing capabilities. In other words, ballistic phonon transport at room temperature has been considered negligible at room temperature. Only recently, novel experiments have demonstrated strong presence of ballistic phonon transport at room temperature through ultrafast X-ray beams,[16] transient thermal gratings,[17] and homogeneously alloyed nanowires.[5] Chang et al.[5] utilized an alloy filtering mechanism for high-frequency phonons in SiGe nanowires and successfully showed
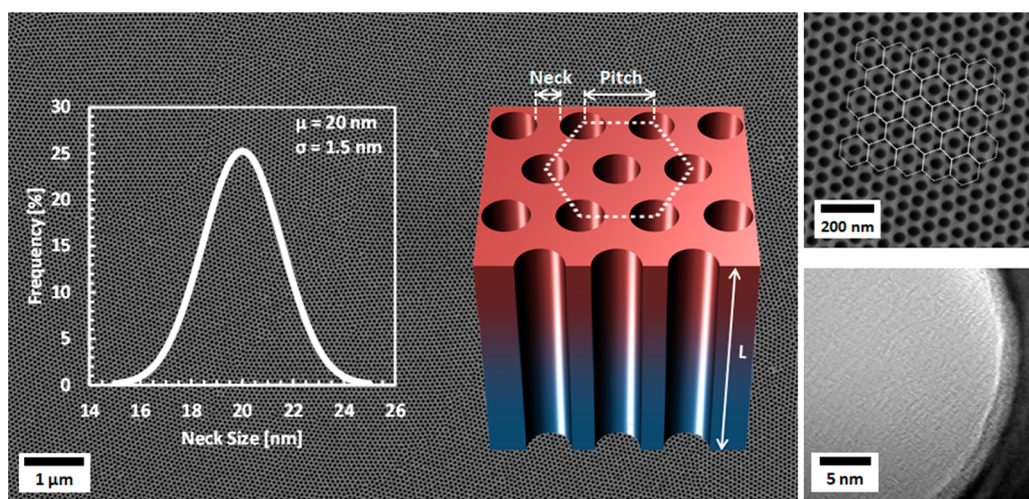
Figure 1. Holey silicon nanostructures fabricated by block copolymer lithography. (a) PS-*b*-P2VP block copolymer, with controlled chemistry, provides highly ordered 60 nm-pitch nanoholes over a large area (>1 mm²). After the pattern transfer on SOI substrates, a DRIE process creates silicon trenches of varying length (*L*) from 200 nm down to 35 nm. The hole patterns follows a normal distribution of 20 ± 1.5 nm neck size and 41 nm ±1.9 nm hole diameter. (b) SEM image shows holey silicon with uniform patterning in hexagonal lattice. (c) HRTEM image shows a smooth boundary between the etched silicon and the air gap.
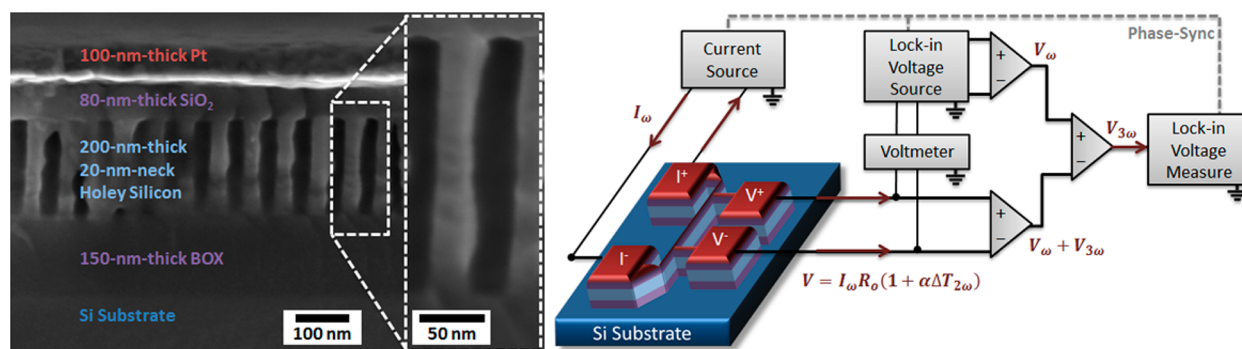

Figure 2. Cross-plane thermal conductivity experimental setup. a, Cross-sectional SEM images show holey silicon trenches that are covered by the sputtered SiO_2 and platinum for thermal conductivity measurements. The etch scallops from the DRIE are undetectable in SEM or TEM, which is likely due to the low aspect ratio (<5) etching process. We further assume that the surface quality of holey silicon is different from that of roughened nanowires investigated in the past studies.[9,13] (b) Schematic of the experimental setup using the 3ω method.[20,21] The third-harmonic voltage ($V_{3\omega}$) captures the second-harmonic temperature rise ($\Delta T_{2\omega}$) in the platinum heater, which is a function of the thermal properties of the underlying materials. Differential measurements of holey silicon devices and silicon thin film devices provide the necessary information to obtain the intrinsic thermal conductivity of holey silicon.

the low frequency driven ballistic thermal conductivity in the range of 1–8 *μ*m. However, the ballistic thermal conductivity data for single-crystalline silicon, particularly in the length scale of 10−100 nm, is not available despite its direct relevance to nanoscale transistors and potential phononic devices. The experimental demonstration of ballistic phonon transport in silicon nanostructures imposes great challenges. For silicon nanowires, the challenge lies at the MEMS device fabrication, in which the spatial resolution typically exceeds the phonon mean free path. For silicon thin films, the challenge lies at the measurement sensitivity, which is typically very low due to the large thermal conductivity of silicon. While the literature is rich with the thermal conductivity data for silicon thin films in the in-plane direction,[18,32,33] the cross-plane thermal conductivity still lacks length (thickness) dependence data. Here we utilize an inverse-nanowire system, i.e., holey silicon, to study ballistic phonon transport and characterize the cross-plane thermal conductivity in the length scale of 35−200 nm. Holey silicon has very low effective thermal conductivity due to porosity and

provides substantially increased sensitivity for cross-plane measurements. The holey silicon nanostructures have demonstrated great potential as thermoelectric materials,[11,12] and our results showing strong ballistic phonon transport may have important implications for the future of phononic applications.

We fabricated holey silicon devices using highly ordered block copolymer (Figure 1). First, we prepared thickness-varying silicon layers from 200 to 35 nm in silicon-on-insulator (SOI) wafers by consuming silicon via thermal oxidation and subsequently etching the oxide in buffered hydrofluoric acid. We then coated the wafers with PS-*b*-P2VP polymer and annealed them in solvent for a sufficient time to create 60 nm pitch self-assembled holes.[14] After evaporating a thin layer of chromium for protecting the polymer pattern, a deep reactive ion etching process created vertical trenches with the aspect ratio up to 5 (Figure 2). Controlled etching recipes provided the hole diameter of 40 ± 2 nm and the neck size of 20 ± 2 nm in multiple samples of varying thickness. In order to heal surface defects that were possibly created during the etching

process, we postannealed the samples at 800 °C in argon. The holey silicon structures were covered by a thin film of sputtered SiO$_2$, and then four-probe platinum electrodes were fabricated using a standard photolithography process. Using the platinum as a mask, we then removed the SiO$_2$ and the holey silicon outside the electrode area using anisotropic dry etching processes. This created a one-dimensional structure on silicon substrate for cross-plane thermal conductivity measurements (Figure 2). Additional fabrication details are in the Supporting Information.

We characterize the cross-plane thermal conductivity of holey silicon using the 3ω method.[20,21] When a platinum electrode transmits current at frequency ω ($I_\omega = I_0 \cos(\omega t)$), Joule heating occurs at 2ω ($Q_{2\omega}$) because the heating power is $I_\omega^2 R = I_0^2 R(1 + \cos(2\omega t))/2$. Consequently, the temperature oscillates at 2ω, and the temperature dependent electrical resistance also has a component at 2ω ($R_{2\omega}$). The resultant voltage drop across the heater now contains a 3ω component ($V_{3\omega} = I_\omega R_{2\omega}$). A circuitry of differential amplifiers and lock-in amplifiers captures the in-phase 3ω voltage with high sensitivity. The measured 3ω voltage is directly related to the temperature oscillation in the platinum heater, which is a function of thermal properties of underlying materials including the holey silicon layer. We fit the data to a multilayer heat conduction solution that accounts for the thermal conductivity, the anisotropy ratio, the boundary resistance, and the heat capacity of each layer using recursive matrix formulation.[21] We maximize the measurement sensitivity to the cross-plane thermal conductivity of holey silicon by optimizing the heating frequency, forcing the heat conduction in one-dimensional, and minimizing the uncertainty in other materials using control devices. The control devices are identical to holey silicon devices except for the absence of holes and provide the information about SiO$_2$ layers and Si substrates for determining the thermal conductivity of holey silicon. This is based on the assumption that holey silicon and control devices share the same thermal properties in the SiO$_2$ layers and the Si substrate. The SiO$_2$ layers are created on both holey silicon and thin film control devices simultaneously inside the same chamber, and we assume any geometric effects such as phonon crowding are negligible in the sputtered SiO$_2$ because the phonon mean free path is very small in the amorphous material. The difference in the cross-sectional areas of holey silicon and thin film control devices are treated with the measured porosity from the image processing characterization. Another assumption is in using a theoretical thermal conductivity for silicon films in control devices, but the uncertainty is low because the silicon films have a very small contribution (<2%) to the total resistance. The sensitivity to holey silicon increases further when the porosity is higher because the effective thermal resistance of holey silicon increases compared to other materials. For porosity 30% or higher, the uncertainty in differential analysis is 6% or lower. Additional experimental details are given in the Supporting Information.

Figure 3 shows the length dependent thermal conductivity of holey silicon at room temperature. The thermal conductivity increases with the length from 1.5 ± 0.2 to 2.8 ± 0.4, 3.9 ± 0.6, and 7.5 ± 1.5 W m^{-1} K^{-1} for 35 to 70, 100, and 200 nm, respectively. The reported values are the material thermal conductivity that is numerically independent of the boundary resistance and the porosity. The porosity values ranging from 20% to 40% are obtained from the image processing method. The strong length dependence indicates that ballistic phonon
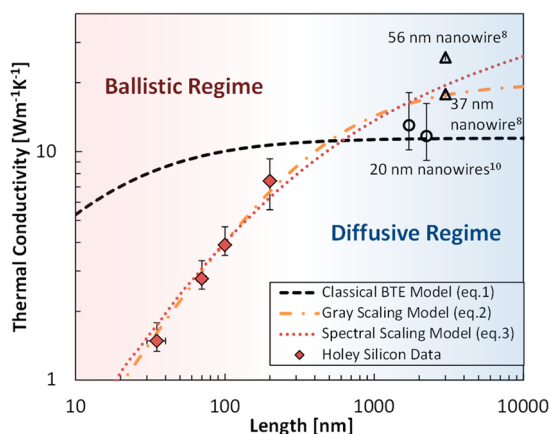

Figure 3. Length dependent thermal conductivity of holey silicon at room temperature. The thermal conductivity values are numerically independent of the boundary resistance and the porosity. The strong length dependence indicates that ballistic phonon transport dominates heat conduction in the length scale of 35−200 nm. A simple scaling model (eq 2) using the average mean free path of bulk silicon predicts the thermal conductivity may approach the reported nanowire data[8] in the infinitely long limit. A semiempirical model (eq 3) accounting for the phonon spectral dependence attributes the length dependent data to the presence of long-wavelength phonons that have the mean free path greater than the length of holey silicon nanostructures.

transport dominates heat conduction in the cross-plane direction of holey silicon. The presence of ballistic phonons in the length scale of 35−200 nm is not surprising because the phonon mean free path in silicon can range up to several micrometers.[25,26] It is, however, important to note that the holey silicon has lateral dimensions as narrow as 20 nm. While classical models predict the smallest dimension regardless of heat flow direction limits phonon transport, the experimental data suggests the length scale that is not the smallest dimension but in the same direction with heat flow can be important.

In general, the Boltzmann transport equation (BTE) is a great resource to understand phonon transport in semiconductors. The thermal conductivity can be expressed in spherical coordinates as,

$$\kappa = \frac{1}{8\pi^2} \sum_n \int_0^{k_o} \int_0^{2\pi} \int_0^{\pi} C_{ph} v_g^2 \tau k^2 \sin\theta \, \mathrm{d}\theta \, \mathrm{d}\phi \, \mathrm{d}k \tag{1}$$

where the heat capacity (C_{ph}), group velocity (v_g), and relaxation time (τ) are each dependent on the phonon dispersion relations (ω, k). The relaxation time due to cross-plane boundary scattering is $L/(2\,v_{ph}\cos\theta)$ where $v_{ph} = \partial\omega/\partial k$. The modeling details are in the Supporting Information. In the worst-case scenario, phonons scatter completely diffusely at the lateral boundaries and the mean free path is limited by the neck size, as if they are passing through nanowires of the diameter equivalent to the neck size. The nanowire analogy provides the classical lower bound for the holey silicon nanostructures (Figure 3).

The length dependent thermal conductivity in silicon nanostructures, while not easily observed in experiment, has been investigated by many theoretical studies.[22−25] One popular approach is using a gray model, which has been reported to reproduce the values from the Green−Kubo calculations[22] and used to study the size effect in the thermal conductivity of silicon nanostructures.[22,25] The thermal conductivity scaling in gray model can be expressed as
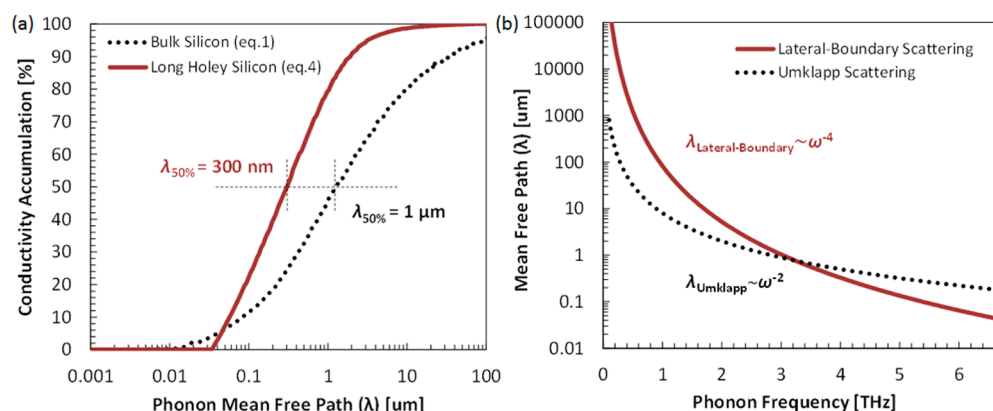
Figure 4. Phonon mean free path calculations. The thermal conductivity accumulation plots (a) show that the median mean free path ($\lambda_{50\%}$) in bulk silicon is about 1 μm and that in the holey silicon of infinite length is about 300 nm. This implies that ballistic phonon transport dominates heat conduction for the holey silicon in the length scale of 35−200 nm. The frequency dependent mean free path calculations for the holey silicon (b) show that the lateral boundary scattering scales by ω^{-4}, like Rayleigh scattering, and the lower frequency phonons can travel greater length despite the presence of surface disorder. This implies that specular scattering by low frequency phonons might be responsible for the length dependent thermal conductivity of the holey silicon.

$$\kappa_{gray} = \kappa_\infty \left(1 + \frac{\lambda_\infty}{L/2} \right)^{-1} \tag{2}$$

where κ_∞ and λ_∞ are the thermal conductivity and phonon mean free path of an infinitely long system. This requires information about the average mean free path as a fitting parameter. The average mean free path estimation based on the kinetic theory ($\lambda = 3\kappa/Cv$) is about 40 nm for bulk silicon, but this method grossly underestimates heat conduction at room temperature. Not all phonons contribute equally to heat conduction because the most phonon population is near the zone boundary and optical phonons have substantially small group velocity compared to acoustic phonons. The average mean free path accounting for the spectral dependence ($\lambda = 3\kappa/\int Cv \, d\omega$) is about 200 nm.[1,25] The average mean free path that best matches the data for silicon thin films[18] and VLS silicon nanowires[19] is also reported as 200−300 nm. By using the average mean free path of 200 nm and the gray model (eq 2), the thermal conductivity in the infinity converges to 20 W m^{-1} K^{-1}, which closely matches the reported data for the 37 nm-wide VLS nanowire.[6] The thermal conductivity prediction in the infinitely long limit also agrees well with a classic modeling of periodic nanoporous silicon[2] and our BTE solution for a nanowire. These imply that the phonon transport in the inverse nanowire holey silicon system resembles that in nanowires of the equivalent cross-sectional area.

While the gray scaling model (eq 2) captures the holey silicon data with the use of average mean free path, a number of recent studies emphasize the use of frequency dependent modeling and accounting for the broad spectrum of phonons in silicon.[17,24−26] For bulk silicon at room temperature, phonons with the mean free path greater than 1 μm contributes about 50% of heat conduction (Figure 4). The median mean free path is several factors larger than the average mean free path, and this provides a more complete picture in analyzing the thermal conductivity size effect. A spectral scaling model accounting for the frequency (ω) dependence of the phonon mean free path can be express as,

$$\kappa_{spectral} = \int_0^{\omega_o} \kappa_\infty(\omega) \left(1 + \frac{\lambda_\infty(\omega)}{L/2} \right)^{-1} d\omega \tag{3}$$

This requires functional forms of the thermal conductivity and the mean free path in the infinitely long system. As mentioned earlier, the classical modeling based on the BTE (eq 1) cannot explain the length dependence in holey silicon because the mean free path is limited by the neck size. We find the mean free path in holey silicon can be greater than the neck size in the modeling framework developed by Murphy et al.[27] and Chen et al.,[8] which is based on the Landauer formalism

$$\kappa_\infty(\omega) = \frac{L}{A} \frac{k_B}{2\pi} \int_0^{\omega_o} \left(\frac{N_1}{1 + L/l} + \frac{N_2}{1 + L/d} \right)$$
$$\frac{X^2 \exp(X)}{(\exp(X) - 1)^2} \, d\omega \tag{4}$$

where L is the length, A is the cross-sectional area, d is the diameter, l is the frequency dependent mean free path, N_1 is the number of modes with the mean free path l, and N_2 is the number of modes with the mean free path limited to d, and $X = \hbar\omega/k_B T$. This model accounts for specular scattering by long wavelength phonons, which have the mean free path scaling by ω^{-4}, and predicts their contribution increases in nanowires with smaller diameter.[8,27] The frequency dependence ($l \sim \omega^{-4}$) resembles that of Rayleigh scattering, and the model treats surface disorder as a collection of point-like impurities. Additional modeling details are in the Supporting Information. Although the original model was developed in the ballistic limit, here we have included Umklapp scattering and applied the cutoff frequency suggested by Mingo[28] to obtain the effective mean free path contributions (Figure 4). Combining the Landauer model (eq 4) and the spectral scaling model (eq 3), we can explain the scaling trend (Figure 3) without using the bulk thermal conductivity or the average mean free path as a fitting parameter. The spectral scaling model predicts the thermal conductivity in the infinity approaches a higher value than the prediction based on the gray model. This is because the Landauer model accounts for long-wavelength phonons that are specularly scattering with lateral boundaries. The transition from ballistic to diffusive transport also occurs at a larger length scale (∼300 nm). This implies that the long-wavelength phonons could be responsible for the mean free path greater than the neck size and the strong size effect observed in the holey silicon. We could also infer that short

wavelength phonons are effectively filtered by the surface disorder and the ballistic phonon transport is predominantly due to long-wavelength phonons.

The long-wavelength phonons also play an important role in understanding the temperature dependence. Figure 5 shows the
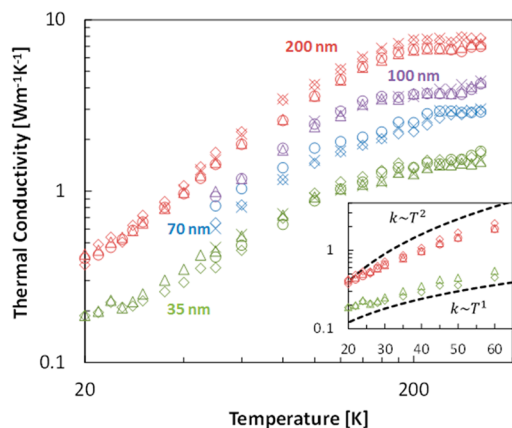

Figure 5. Temperature dependent thermal conductivity of the holey silicon nanostructures. The positive temperature dependence indicates that phonon boundary scattering is dominant throughout the temperature range presented here. The low temperature thermal conductivity data at 20−60 K deviate from the classical prediction ($k \sim T^3$) that follows the temperature dependence governed by the heat capacity. The Landauer modeling (eq 4) attributes the nonclassical low temperature dependence to the frequency dependence of phonon boundary scattering,[27] and our experimental results support the prediction of having specular phonons in narrow silicon nanostructures with limiting feature sizes down to 20 nm. While the lateral boundary scattering might be partially specular, the vertical boundary scattering might be completely diffuse and dictate the length dependent thermal conductivity in the holey silicon.

temperature dependent thermal conductivity of holey silicon down to 20 K. At cryogenic temperatures, or when the dominant phonon wavelength is greater than the size of impurities, the thermal conductivity should scale by the power of 3 ($k \sim T^3$), based on the classical law for heat capacity. However, the holey silicon thermal conductivity data in the range of 20−60 K show the temperature dependence scaling by the power of 2 ($k \sim T^2$). This nonclassical observation is not new for silicon nanowires. Li et al.[8] and Chen et al.[10] showed VLS nanowires of diameter in the range 20−40 nm exhibit unusual temperature dependence ($k \sim T^{1-2}$) at low temperatures (20−60 K). One perspective is to consider quantum confinement effect, which changes phonon dispersion relation.[29] However, other studies argue the confinement effect is only relevant for temperatures below 10 K because roughness destroys coherence for short-wavelength phonons.[30,31] Another perspective is to consider increased contribution of surface disorder and account for frequency boundary scattering,[27] which is consistent with our explanation for the ballistic transport at room temperature. The combined contributions of specular and diffusive transport depending on the phonon frequency with respect to the length scale of surface disorder can result in the low temperature thermal conductivity deviating from the classical dependence.

The thermal conductivity data and the scaling models presented here have great implications for thermoelectric applications.[14,15] Tang et al.[14] demonstrated the block copolymer patterned holey silicon can have the thermoelectric

figure of merit (ZT) up to 0.4 at room temperature. Our cross-plane data is directly applicable for planar devices where temperature gradients occur across layers. Holey silicon nanostructures are also more attractive in such integrated systems compared to nanowire arrays because of mechanically and electrically stable contact qualities. One of major technological challenges for holey silicon thermoelectric devices would be scaling up to higher-aspect-ratio structures while keeping the thermal conductivity low. The scaling models predict that the thermal conductivity might reach a plateau when the length is sufficiently larger than the phonon mean free path. Past studies on the roughness suggest the phonon mean free path in silicon can be strongly suppressed by various methods of surface treatment.[7−11] For instance, the electroless etching method[9] has demonstrated a successful reduction of the thermal conductivity by creating surface roughness on the order of 1−5 nm. In such roughened holey silicon systems, the transition from ballistic to diffusive transport would happen in a shorter length scale, which would be more favorable for thermoelectric applications. The results here also suggest that keeping the neck size small is important. Ongoing development of etching process can shed light on fabricating higher-aspect-ratio holey silicon nanostructures, which may become a commercially viable thermoelectric material particularly at high temperatures.

The silicon thermal conductivity data in the length scale of 35−200 nm has immediate implications for nanoscale electronic systems. With the rapid scaling trend in transistors, heat generation in reduced geometry is of ever-increasing importance for both device performance and reliability. We expect the thermal conductivity of silicon to scale linearly down with the reduced dimension in transistors. The ballistic phonon transport would be responsible for hotspots in nanoscale systems and the heat generation would be beyond the predictions based on classical size effect models.

Although the impact is not as immediate as on electronic applications, the observed room-temperature ballistic phonon transport in the holey silicon nanostructures is very promising for potential phononic applications. Our work suggests that thermal diodes or potential phononic waveguides can benefit from the persistent long-wavelength phonons in silicon nanostructures even when the limiting dimension is down to 20 nm with fabrication involving conventional etching processes. Surface engineering that filters high-frequency phonons and increases the contribution of low-frequency phonons could provide new pathways for manipulating phonons and controlling heat flows. We expect that the scaling trend of transistors would be more favorable for potential integration of nanoelectronics and phononics because the mean free path of long-wavelength phonons exceeds typical dimensions of commercial transistors. The fact that silicon has excellent electrical and thermal properties is a great advantage for the development of phononic devices. Holey silicon nanostructures, with strong ballistic phonon transport as presented here, show potential to become a building block of future phononic systems.

The fundamentals of heat transfer governed by the Fourier law break down at the nanoscale, specifically when the length scale is smaller than the carrier mean free path. This work provides self-consistent experimental data sets for holey silicon in the length scale below the average phonon mean free path of bulk silicon. The scaling models show the length dependent thermal conductivity could be due to specular scattering in

lateral boundaries by long wavelength phonons. The frequency dependent boundary scattering could be responsible for both the unique size effect and the nonclassical temperature dependence of the holey silicon. These results are particularly important for managing heat generation in silicon transistors that are scaling much below the phonon mean free path. The holey silicon is providing pathways for engineering the thermal conductivity in silicon nanostructures, which can lead to cost-effective thermoelectric devices and could potentially be a breakthrough for phononic devices.

■ ASSOCIATED CONTENT

⑤ Supporting Information

Device fabrication and sample preparation for TEM and Raman spectroscopy details, additional SEM images of the holey silicon, Raman spectroscopy results, thermal conductivity modeling details, and additional figures for the holey silicon data. This material is available free of charge via the Internet at http://pubs.acs.org.

■ AUTHOR INFORMATION

Corresponding Author
*(P.Y.) E-mail: p_yang@berkeley.edu.

Author Contributions
[#]The manuscript was written through contributions of all authors. All authors have given approval to the final version of the manuscript. These authors contributed equally.

Notes
The authors declare no competing financial interest.

■ ACKNOWLEDGMENTS

■ REFERENCES

(1) Chen, G. Thermal conductivity and ballistic-phonon transport in the cross-plane direction of superlattices. *Phys. Rev. B* **1998**, *57*, 14958−14973.

(2) Yang, R.; Chen, G.; Dresselhaus, M. S. Thermal conductivity of simple and tubular nanowire composites in the longitudinal direction. *Phys. Rev. B* **2005**, *72*, 125418−125425.

(3) Sverdrup, P. G.; Sinha, S.; Asheghi, M.; Srinivasan, U.; Goodson, K. E. Measurement of ballistic phonon conduction near hotspots in silicon. *Appl. Phys. Lett.* **2001**, *78*, 3331−3333.

(4) Pop, E.; Sinha, S.; Goodson, K. E. Heat generation and transport in nanometer-scale transistors,. *Proc. IEEE* **2006**, *94*, 1587−1601.

(5) Hsiao, T.-K.; Chang, H.-K.; Liou, S.-C.; Chu, M.-W.; Lee, S.-C.; Chang, C.-W. Observation of room-temperature ballistic thermal conduction persisting over 8.3 μm in SiGe nanowires. *Nat. Nanotechnol.* **2013**, *8*, 534−538.

(6) Li, N.; Ren, J.; Wang, L.; Zhang, G.; Hänggi, P.; Li, B. Manipulating heat flow with electronic analogs and beyond. *Rev. Mod. Phys.* **2012**, *84*, 1045−1066.

(7) Martin Maldovan. Sound and heat revolutions in phononics. *Nature 503* (**2013**): 209−217.

(8) Li, D.; Wu, Y.; Kim, P.; Shi, L.; Yang, P.; Majumdar, A. Thermal conductivity of individual silicon nanowires,. *Appl. Phys. Lett.* **2003**, *83*, 2934−2936.

(9) Hochbaum, A. I.; Chen, R. K.; Delgado, R. D.; Liang, W. J.; Garnett, E. C.; Najarian, M.; Majumdar, A.; Yang, P. D. Enhanced thermoelectric performance of rough silicon nanowires. *Nature* **2008**, *451*, 163−167.

(10) Chen, R.; Hochbaum, A. I.; Murphy, P.; Moore, J.; Yang, P.; Majumdar, A. Thermal Conductance of Thin Silicon Nanowires. *Phys. Rev. Lett.* **2008**, *101*, 105501−105505.

(11) Boukai, A. I.; Bunimovich, Y.; Tahir-Kheli, J.; Yu, J.-K.; Goddard, W. A., III; Heath, J. R. Silicon nanowires as efficient thermoelectric materials. *Nature* **2008**, *451*, 168−171.

(12) Hippalgaonkar, K.; Huang, B.; Chen, R.; Sawyer, K.; Ercius, P.; Majumdar, A. Fabrication of Microdevices with Integrated Nanowires for Investigating Low-Dimensional Phonon Transport. *Nano Lett.* **2010**, *10*, 4341−4348.

(13) Lim, J.; Hippalgaonkar, K.; Andrews, S. C.; Majumdar, A.; Yang, P. Quantifying surface roughness effects on phonon transport in silicon nanowires. *Nano Lett.* **2012**, *12*, 2475−2482.

(14) Tang, J.; Wang, H.-T.; Lee, D. H.; Fardy, M.; Huo, Z.; Russell, T. P.; Yang, P. Holey Silicon as an Efficient Thermoelectric Material. *Nano Lett.* **2010**, *10*, 4279−4283.

(15) Yu, J.-K.; Mitrovic, S.; Tham, D.; Varghese, J.; Heath, J. R. Reduction of Thermal Conductivity in Phononic Nanomesh Structures. *Nat. Nanotechnol.* **2010**, *5*, 718−721.

(16) Siemens, M. E.; Li, Q.; Murnane, M. M.; Kapteyn, H. C.; Yang, R. G.; Nelson, K. A. Quasi-ballistic thermal transport from nanoscale interfaces observed using ultrafast coherent soft X-ray beams. *Nat. Mater.* **2010**, *9*, 26−30.

(17) Johnson, J. A.; Maznev, A. A.; Cuffe, J.; Eliason, J. K.; Minnich, A. J.; Kehoe, T.; Torres, C. M. S.; Chen, G.; Nelson, K. A. Direct Measurement of Room-Temperature Nondiffusive Thermal Transport Over Micron Distances in a Silicon Membrane. *Phys. Rev. Lett.* **2013**, *110*, 025901−025906.

(18) Ju, Y. S.; Goodson, K. E. Phonon scattering in silicon films with thickness of order 100 nm. *Appl. Phys. Lett.* **1999**, *74*, 3005−3007.

(19) Ju, Y. S. Phonon heat transport in silicon nanostructures. *Appl. Phys. Lett.* **2005**, *87*, 153106/1−153106/3.

(20) Cahill, D. G. Thermal conductivity measurement from 30 to 750 K: the 3ω method. *Rev. Sci. Instrum.* **1990**, *61* (2), 802−808.

(21) Lee, J.; Li, Z.; Reifenberg, J. P.; Lee, S.; Sinclair, R.; Asheghi, M.; Goodson, K. E. Thermal conductivity anisotropy and grain structure in Ge$_2$Sb$_2$Te$_5$ films. *J. Appl. Phys.* **2011**, *109*, 084902−084908.

(22) Schelling, P. K.; Phillpot, S. R.; Keblinski, P. Comparison of atomic-level simulation methods for computing thermal conductivity. *Phys. Rev. B* **2002**, *65*, 144306−144328.

(23) Fang, J.; Pilon, L. Scaling laws for thermal conductivity of crystalline nanoporous silicon based on molecular dynamics simulations. *J. Appl. Phys.* **2011**, *110*, 064305−064315.

(24) Sellan, D. P.; Landry, E. S.; Turney, J. E.; McGaughey, A. J. H.; Amon, C. H. Size effects in molecular dynamics thermal conductivity predictions. *Phys. Rev. B* **2010**, *81*, 214305−214315.

(25) Yang, F.; Dames, C. Mean free path spectra as a tool to understand thermal conductivity in bulk and nanostructures. *Phys. Rev. B* **2013**, *87*, 035437−035449.

(26) Henry, A. S.; Chen, G. Spectral phonon transport properties of silicon based on molecular dynamics simulations and lattice dynamics. *J. Comput. Theor. Nanosci.* **2008**, *5*, 1−12.

(27) Murphy, P. G.; Moore, J. E. Coherent phonon scattering effects on thermal transport in thin semiconductor nanowires. *Phys. Rev. B* **2007**, *76*, 155313−155324.

(28) Mingo, N. Calculation of Si nanowire thermal conductivity using complete phonon dispersion relations. *Phys. Rev. B* **2003**, *68*, 113308−113312.

(29) Zou, J.; Balandin, A. Phonon heat conduction in a semi-conductor nanowire. *J. Appl. Phys.* **2001**, *89*, 2932−2938.

(30) Prasher, R.; Tong, T.; Majumdar, A. Approximate analytical models for phonon specific heat and ballistic thermal conductance of nanowires. *Nano Lett.* **2008**, *8*, 99−103.

(31) Dames, C.; Chen, G. Theoretical phonon thermal conductivity of Si/Ge superlattice nanowires,. *J. Appl. Phys.* **2004**, *95*, 682−693.

(32) Liu, W.; Asheghi, M. Thermal Conductivity Measurements of Ultra-Thin Single Crystal Silicon Layers. *J. Heat Transfer* **2006**, *128*, 75−83.

(33) Asheghi, M.; Leung, Y. K.; Wong, S. S.; Goodson, K. E. Phonon-boundary scattering in thin silicon layers,. *Appl. Phys. Lett.* **1997**, *71*, 1798−1800.

G